Ca^{2+}-Dependent Inactivation of a Cloned Cardiac Ca^{2+} Channel α_1 Subunit (α_{1C}) Expressed in *Xenopus* Oocytes

Alan Neely,* Riccardo Olcese,* Xiangyang Wei,* Lutz Birnbaumer,*‡ and Enrico Stefani*§
Departments of *Molecular Physiology and Biophysics, ‡Cell Biology, and §Neurology, Baylor College of Medicine, Houston, Texas 77030 USA

ABSTRACT The α_1 subunit of cardiac Ca^{2+} channel, expressed alone or coexpressed with the corresponding β subunit in *Xenopus laevis* oocytes, elicits rapidly inactivating Ca^{2+} currents. The inactivation has the following properties: 1) It is practically absent in external Ba^{2+}; 2) it increases with Ca^{2+} current amplitudes; 3) it is faster at more negative potentials for comparable Ca^{2+} current amplitudes; 4) it is independent of channel density; and 5) it does not require the β subunit. These findings indicate that the Ca^{2+} binding site responsible for inactivation is encoded in the α_1 subunit and suggest that it is located near the inner channel mouth but outside the membrane electric field.

INTRODUCTION

A number of processes such as neurotransmitter release, muscle contraction, or changes in membrane conductance are initiated by the influx of Ca^{2+} through voltage-activated Ca^{2+} channels (Bean, 1989; Bertolino and Llinas, 1992; Kostyuk, 1992) and are terminated by the concerted action of Ca^{2+} binding proteins, Ca^{2+}-ATPases, and the Na^+/Ca^{2+} exchanger that ensures that cytoplasmic Ca^{2+} is restored to submicromolar concentrations (Kostyuk, 1992; Carafoli, 1993). An additional mechanism contributing to the control of intracellular Ca^{2+} is inactivation of L-type Ca^{2+} channels by Ca^{2+} entering through the channel (Eckert and Chad, 1984; Chad, 1989). This inactivation is evidenced by a fast decay of macroscopic currents in external Ca^{2+} (but not in external Ba^{2+}), by a parallel increase of the rate of decay and Ca^{2+} current amplitude and, in double pulse experiments, by an inverse relationship between the amplitudes of Ca^{2+} currents during the first and second pulses (Brehm and Eckerd, 1978; Tillotson, 1979; Eckert and Tillotson, 1981).

Simple diffusion modeling predicts that Ca^{2+} can reach millimolar concentrations at the inner mouth of the channel a few microseconds after channel opening (Simon and Llinas, 1985; Llinas et al., 1992), yet Ca^{2+}-dependent inactivation develops much more slowly, in tens or hundreds of milliseconds. One proposed explanation for this difference is that even when Ca^{2+} binds rapidly to the channel, the rate of inactivation is limited by the rate at which the channel protein can change its conformation (Sherman et al., 1990; Keizer and Maki, 1992). Alternatively, the slow rate of inactivation may reflect the Ca^{2+} buildup at some distance from the pore (Eckert and Chad, 1984; Standen and Stanfield, 1982). This would be the case if other proteins were involved. For example, inactivation may result from the dephosphorylation of the channel protein by a Ca^{2+}-dependent phosphatase (Chad and Eckert, 1986; Kalman et al., 1988) or from the down-regulation of channel activity by Ca^{2+} acting on cytoskeletal components (Johnson and Byerly, 1993a).

We report here the experimental conditions to study Ca^{2+}-induced inactivation of a cloned cardiac Ca^{2+} channel, and show that inactivation by Ca^{2+} depends on transmembrane Ca^{2+} flow, that Ca^{2+} entry can be more effective at more negative potentials, and that the level of channel expression does not affect the rate of Ca^{2+}-dependent inactivation. Furthermore, Ca^{2+}-dependent inactivation was insensitive to intracellular Ca^{2+} buffer concentrations that effectively suppress the activation of the endogenous Ca^{2+}-activated Cl^- current. Finally, this inactivation was present when the α_1 subunit was expressed without the β subunit, and thus we conclude that the molecular domains for the Ca^{2+}-inactivation are encoded in the cardiac α_1 subunit.

MATERIALS AND METHODS

RNA synthesis and oocyte injection

The cRNAs were prepared from two plasmids bearing the *a*-splice variant of the type C or cardiac α_1 subunit ($\alpha_{1C\text{-}a}$), formerly also CaCh2a, and the type *2a* cardiac β subunit (β_{2a}), here referred to simply as α_1 and β. The α_1 cDNA is linearized with *Hind*III (Wei et al., 1991) and β cDNA with *Not*I (Perez Reyes et al., 1992). Transcription was done at 37°C in a volume of 25 ml containing 40 mM Tris-HCl (pH 7.2), 6 mM $MgCl_2$, 10 mM dithiothreitol, 4 mM spermidine, 0.4 mM each of ATP, GTP, CTP, and UTP, 1 mM 7-methyl GTP, 0.5 mg of linearized DNA template, and 10 units of T7 RNA polymerase (Boehringer Mannheim, Indianapolis, IN). The cRNA products were extracted with phenol/chloroform and recovered by precipitation with ethanol, suspended in double distilled water to a final concentration of 0.2 mg/ml of each species, and 50 nl was injected per oocyte. Before injection, oocytes were defolliculated by collagenase treatment (type I, 2 mg/ml for 40 min at room temperature; Sigma Chemical Co., St. Louis, MO). Oocytes were maintained at 19.5°C in Barth solution. Recordings were done 4 to 12 days after RNA injection.

Received for publication 29 November 1993 and in final form 21 March 1994.

Address reprint requests to Enrico Stefani, Department of Molecular Physiology and Biophysics, Baylor College of Medicine, One Baylor Plaza, Houston, TX 77030-3498. Tel.: 713-798-5725; Fax: 713-798-3474; E-mail: stefani@phy.bcm.tmc.edu.

Dr. Wei's current address: Medical College of Georgia, Institute for Molecular Medicine and Genetics. Augusta, GA 30912.

0006-3495/94/06/1895/09 $2.00

Recording techniques and BAPTA injection

Macroscopic currents were recorded using the cut-open oocyte vaseline gap technique (Taglialatela et al., 1992). Briefly, *Xenopus laevis* oocytes were placed in a perspex chamber consisting of three vertically stacked compartments: 1) a recording pool (top) from which voltage clamped currents are recorded, and 2) a guard pool (middle) that is set at the same voltage as the recording chamber to isolate the top chamber from the 3) current-injecting pool (bottom). The voltage across the membrane enclosed in the top chamber is probed with a glass micropipette and clamped to 0 mV by injecting current through the bottom chamber. A low path resistance to the oocyte interior is established by permeabilizing the membrane exposed to the bottom chamber with 0.1% saponin in internal saline. Signal to noise ratio was enhanced by using large microelectrodes (0.05–0.2 MΩ), a 10 MΩ feedback resistor in the current-voltage converter, and the control amplifiers in the open loop gain configuration. The series resistance originated from the distributed resistance between the tip of the control microelectrode, and the inner surface of the oocyte membrane had typical values of 1 kΩ. The holding potential was −90 mV. Linear components were analogically or digitally subtracted. The digital subtraction was obtained by scaled currents elicited by small negative control pulses of one-fourth the amplitude of the stimulating pulse ($P/-4$). All experiments were carried out at room temperature (22°C). A personal computer-based acquisition system was used. Signals before acquisition were filtered at half or a quarter of the sampling frequency.

The following external solutions were used in the top and guard compartments: 0 Cl/10 Ba, 10 mM Ba^{2+}; 96 mM Na^+; 10 mM HEPES titrated to pH 7.0 with $CH_3(SO_3)^-$; 0 Cl/5 Ca: 5 mM Ca^{2+}; 102 mM Na^+; 10 mM HEPES titrated to pH 7.0 with $CH_3(SO_3)^-$; 96 Cl/10 Ba, 10 mM Ba^{2+}; 96 mM NaCl; 10 mM HEPES titrated to pH 7.0 with $CH_3(SO_3)^-$; 96 Cl/5 Ca, 5 mM Ca^{2+}; 102 mM NaCl; 10 mM HEPES titrated to pH 7.0 with $CH_3(SO_3)^-$. The solutions in the bottom chamber facing the oocyte cytoplasm were either 120 mM TEA (10 mM HEPES; 0.5 mM EGTA, 5 mM $MgSO_4$, titrated to pH 7.0 with $CH_3(SO_3)^-$ (Figs. 2, 3, 4, and 8)) or 110 mM K-glutamate (10 mM HEPES, titrated to pH 7.0 with K(OH) (Figs. 1, 6, and 7)).

Ca^{2+}-dependent Cl^- currents were measured in excised macropatches from control *Xenopus* oocytes. The viteline layer was removed under the microscope with fine forceps after pre-incubating in hyperosmotic solution (Methfessel et al., 1986). Records were obtained with an Axopatch-200 amplifier (Axon Instrument, Foster City, CA). Pipette tip diameters were about 6 mm with a final resistance of about 0.5 MΩ. Stray capacitance was reduced by coating the shank of the pipettes with a mixture of parafilm and light mineral oil. The solution in the pipette was 100 mM KCH_3SO_3, 5 mM NaCl, and 10 mM HEPES at pH 7.0 (KMESCl-5), whereas the bath was either 115 mM KCl (KCl) or 110 mM KCH_3SO_3 (KMES) with 10 mM HEPES titrated at pH 7.0. $CaCl_2$ was added from a stock solution to a final concentration of 50, 100, or 500 mM. Solutions with estimated free Ca^{2+} concentration of 2 and 10 mM contained 5 mM EGTA and 4.2 and 4.8 mM Ca^{2+}, respectively (Fabiato, 1988). Na_4-BAPTA (1,2-bis(*o*-aminophenoxy)ethane-*N*, *N*,*N*′,*N*′-tetraacetate) was loaded into a glass micropipette of a tip diameter of about 20 mm and injected with an automatic microinjector (Drummond, Bromall, PA) immediately before mounting the oocyte in the recording chamber. Na_4-BAPTA stock solutions of 50 mM were made in distilled water at pH 7.0 with 10 mM HEPES-K. To obtain the BAPTA solutions of 5 and 2.5 mM, the BAPTA stock solution was mixed with 110 mM $NaCH_3SO_3$ and titrated to pH 7.0 with K(OH).

RESULTS

Inactivating Ca^{2+} currents expressed in *Xenopus* oocytes

Because prominent Ca^{2+}-activated Cl^- currents in *Xenopus* oocytes (Miledi, 1982; Barish, 1983) contaminate Ca^{2+} currents when Ca^{2+} is used as the charge carrier, in this first series of experiments we sought to find conditions that eliminate Ca^{2+}-activated Cl^- currents when using the cut-open oocyte voltage-clamp (COVG) technique (Taglialatela et al., 1992). Fig. 1 shows inward currents recorded from oocytes injected with the α_1 ($\alpha_{1C\text{-}a}$) (Wei et al., 1991) and β (β_2) (Perez-Reyes et al., 1992) subunit cRNAs of the cardiac Ca^{2+} channel. Currents in Fig. 1 *A* were recorded in Cl^--free external solution with 10 mM Ba^{2+} (0 Cl/10 Ba). The corresponding peak current-voltage relationship is shown in Fig. 1 *G* (△). The current-voltage relationship of peak Ba^{2+} currents is bell-shaped with a reversal potential positive to +50 mV, which is expected for Ba^{2+} currents going through Ca^{2+} channels. However, deactivation tail currents recorded at the end of depolarizing pulses are slow, and their time constant increases with the size of the inward Ba^{2+} current during the pulse. This suggests that these Ba^{2+} currents are contaminated by the outward movement of Cl^-. Using Cl^- in the external solution (96 Cl/10 Ba) resulted in the activation of outward currents (Fig. 1 *B*), and as expected for Ca^{2+}-dependent Cl^- currents, replacing 10 mM Ba^{2+} by 5 mM Ca^{2+} (96 Cl/5 Ca, Fig. 1 *C*) greatly potentiates these currents. The peak current-voltage plot in Ba^{2+} with external Cl^- was typically N-shaped (Fig. 1 *G*, in 96 Cl/10 Ba), indicating that the influx of Ba^{2+} activates Cl^- currents. Furthermore, in inside-out patch-clamp records, we have confirmed that this Cl^- conductance can be activated by Ba^{2+}

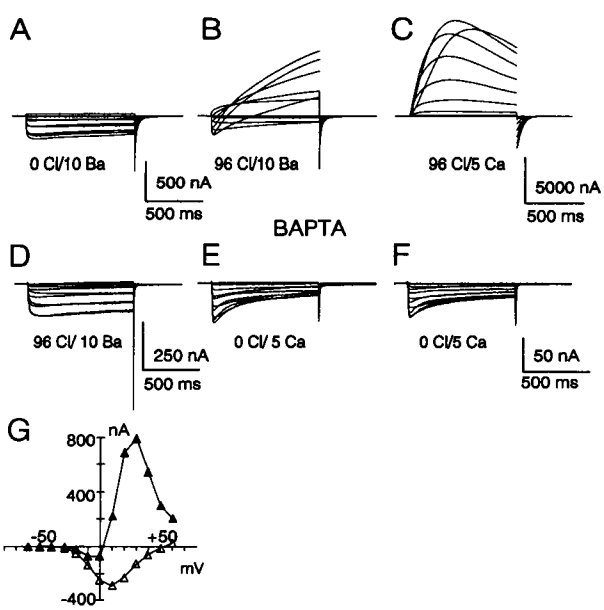

FIGURE 1 Ca^{2+} and Ba^{2+} currents can be contaminated by Cl^- currents. Superimposed voltage clamp traces during 1 s depolarizing pulses from a non-BAPTA-injected oocyte (*A–C*) and a BAPTA-injected oocyte (*D–F*) expressing α_1 and β subunits. Membrane currents for the non-BAPTA-injected oocyte were recorded in 0 Cl/10 Ba (*A*), in 96 Cl/10 Ba (*B*), and in 96 Cl/5 Ca(*C*). For the BAPTA-injected oocytes, currents were recorded in 0 Cl/10 Ba (*D*), in 96 Cl/5 Ca (*E*) and in 0 Cl/5 Ca (*F*). Current-voltage plot in *G* for peak inward currents from *A* (△) and outward currents measured at the end of the pulse from *B* (▲). Holding potential was −90 mV, and depolarizing steps were from −60 to +60 mV in 10-mV increments. Linear components were subtracted by the P/−4 subpulse method from the holding potential. (*D–F*) 37 nl of 50 mM BAPTA$(Na)_4$ was injected. Files: *A* E1325C02; *B* E31225C03; *C* E31225C04; *D* J3125C14; *E* J3125C06; *F* J3125C04.

(see below). Therefore, even in the absence of external Cl^- and with Ba^{2+} as the charge carrier, inward currents can be contaminated by the outward movement of Cl^-. This contamination is more prominent during tail current measurements at negative potentials due to the large outward driving force for intracellular Cl^-.

Previous reports have shown that activation of oocyte Cl^- channels, either by Ca^{2+} going through Ca^{2+} channels or by exposure to a Ca^{2+} ionophore, can be suppressed by injection of the Ca^{2+} buffer EGTA (Miledi and Parker, 1984; Boton et al., 1989). Similarly, we found that the injection of the Ca^{2+} buffer BAPTA prevents the activation of Cl^- currents in oocytes expressing cardiac Ca^{2+} channels. Fig. 1, *D* and *E* show inward Ba^{2+} and Ca^{2+} current from an oocyte injected with 37 nl of 50 mM BAPTA (~1850 pmol) recorded in the presence of external Cl^-. With intracellular BAPTA, even in the presence of extracellular Cl^-, there are no outward currents during the pulse, and deactivation tail currents are fast (Fig. 1 *D*), indicating that currents are no longer contaminated by Cl^- influx. This was further confirmed by a more stringent test in which replacement of external Cl^- with the nonpermeant anion methanesulphonate (0 Cl/5 Ca, Fig. 1 *F*) left inward Ca^{2+} currents unaltered. In conclusion, these experiments indicate that unless internal free Ca^{2+} is reduced by a Ca^{2+} buffer, Ba^{2+} as well as Ca^{2+} currents can be contaminated by the activation of endogenous Cl^- currents, which can take place even in the absence of external Cl^-. In these conditions inward Ca^{2+} currents are not maintained during the pulse, unmasking a Ca^{2+} dependent inactivation process.

Inactivation of expressed Ca^{2+} channels is dependent on Ca^{2+} current amplitude

Records in Fig. 1, *D* and *E* show that during prolonged depolarization, inward currents spontaneously decay in external Ca^{2+} but not Ba^{2+}, indicating that expressed cardiac Ca^{2+} channels undergo Ca^{2+}-dependent inactivation that persists in BAPTA-injected oocytes. This process is illustrated in Fig. 2 on BAPTA-injected oocytes coexpressing α_1 and β subunits in which we studied the relationship between Ca^{2+} current amplitude and the rate of Ca^{2+} decay during the pulse and the effect of replacing Ca^{2+} by Ba^{2+}. The Ca^{2+} current amplitude was varied by changing either the pulse potential or the external Ca^{2+} concentration.

The records in the left panel of Fig. 2, obtained in 5 mM external Ca^{2+}, show the positive relationship between the amplitude of the current and its rate of decay. In *A*, the peak current amplitude increases with depolarization up to 10 mV, and the rate of decay becomes progressively faster, whereas in *B*, the Ca^{2+} current amplitude decreases for depolarizations larger than 10 mV and the rate of decay becomes progressively slower. This observation indicates that the rate of Ca^{2+} current decay during the pulse is directly related to the Ca^{2+} current amplitude. When 5 mM external Ca^{2+} was replaced by 10 mM external Ba^{2+} (*C* and *D*; 0 Cl/10 Ba), the current decay during the pulse was greatly slowed. The slow

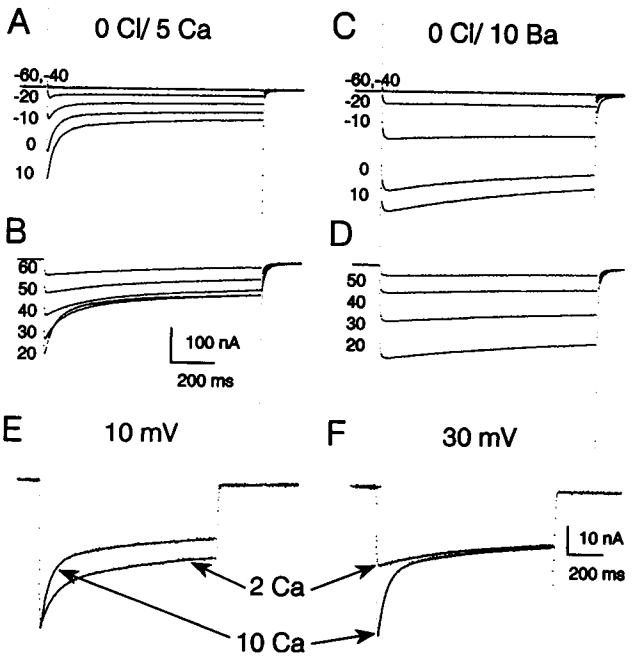

FIGURE 2 The rate of Ca^{2+} current decay is dependent on the peak Ca^{2+} current amplitude and voltage. (*A–D*) Current recordings during 1 s depolarizing steps to the voltage indicated to the left of each trace. Currents were first recorded in 0 Cl/5 Ca (*A*, *B*) and then in 0 Cl/10 Ba (*C*, *D*). Holding potential was −90 mV, and pulses had 10 mV voltage increments. *A* and *C* show voltages evoking currents of increasing amplitudes, whereas *B* and *D* of decreasing amplitudes. Traces were analogically subtracted for linear resistive components. *E* and *F* show the effect of increasing external Ca^{2+} from 2 to 10 mM on the rate of inactivation for a step to 10 (*E*) and 30 (*F*) mV. The traces show superimposed data points and fitted curves to the sum of two exponentials of the form $A_f \cdot \exp(-t/t_f) + A_s \cdot \exp(-t/t_s) + P$, where A_f and A_s are the amplitude factors, t_f and t_s are the time constants, and P is the offset. The subscripts *s* ands *f* stand for fast and slow components, respectively. In 2 mM Ca^{2+} t_f was 69 and 514 ms for 10 and 30 mV, whereas in 10 mM Ca^{2+} the corresponding values were 45 and 69 ms, respectively. The slow component t_s was little affected by the pulse potential and external Ca^{2+}. These traces were digitally subtracted by the *P*/−4 protocol. Oocytes were expressing $\alpha_1\beta$ subunits and were injected with 37 nl of 50 mM BAPTA$(Na)_4$. Files: *A* and *B* B2625C03; *C* and *D* B2625C07; *E* and *F* C327C02 and C327C04.

decay in the presence of external Ba^{2+} can be attributed to a slow voltage-dependent inactivation process normally found in L-type Ca^{2+} channels (Lee et al., 1985; Hadley and Hume, 1987; Campbell et al., 1988; Hadley and Lederer, 1991; Gutnick et al., 1989; Giannattasio et al., 1991; Castellano et al., 1993). In this study we shall focus on the initial rate of the Ca^{2+} current decay, which reflects the Ca^{2+}-dependent inactivation process.

The Ca^{2+} dependency of inactivation was further established by the increase in the rate of current decay after raising external Ca^{2+} from 2 to 10 mM (Fig. 2, *E* and *F*). At 10 mV (*E*), the rise in external Ca^{2+} did not increase the peak current amplitude but accelerated Ca^{2+} current decay. The initial rate of inactivation increased from 0.014 ms^{-1} in 2 mM Ca^{2+} to 0.022 ms^{-1} in 10 mM Ca^{2+}. This result indicates that the rate of inactivation relates to the amplitude of the single channel current rather than to the peak of the macroscopic currents,

because the amplitude of single channel current should increase with external Ca^{2+} concentrations. Peak currents remain the same in this experiment because raising external Ca^{2+} also results in a right-shift in the voltage dependence of the probability of channel opening (P_o), which offsets the increase in single channel current. The records in Fig. 2 *F* show the effect of raising external Ca^{2+} during a pulse to +30 mV. At this potential, raising external Ca^{2+} is expected to have a greater effect on single channel current amplitude than on the channel P_o since the latter is expected to be closer to saturation and, therefore, will be affected to a lesser extent by surface charges. As predicted, the difference in the rate of current decay between 2 mM and 10 mM Ca^{2+} is even larger.

Inactivation of expressed Ca^{2+} channels is dependent on the preceding Ca^{2+} entry in double pulse experiments

For a Ca^{2+}-dependent inactivation process, it is expected that in double pulse experiments, the amplitude of the current during the second constant test pulse should be inversely related to the current evoked by the preceding pulse. Fig. 3 shows one experiment in an oocyte coexpressing α_1 and β subunits and injected with BAPTA. The current traces and the corresponding voltage protocol are shown in *A*. The peak current amplitudes for pre-pulses and test pulses versus the pre-pulse voltage are plotted in *B*. As expected for a current-mediated inactivation, the magnitude of the inward current during the test pulse goes through a minimum when the current of the prepulse is at its maximum and then is restored for large pre-pulse potentials near or above the Ca^{2+} reversal potential (Eckert and Tillotson, 1981; Standen and Stanfield, 1982).

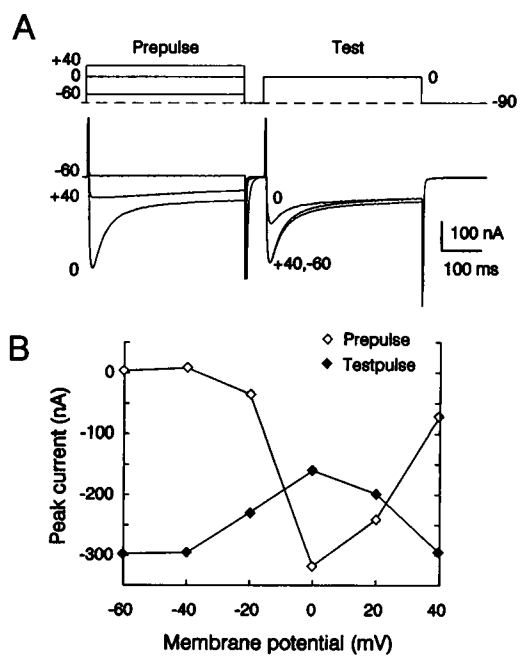

FIGURE 3 Double-pulse experiments demonstrate Ca^{2+} current dependence of inactivation. (*A*) Stimulation protocol and current traces for three amplitudes of prepulses: below detection (−60 mV), evoking maximal current (0 mV), and near the reversal potential (+40 mV). The second pulse was constant to 0 mV. (*B*) Peak current voltage relationship for the prepulse (◇) and for the current during the second test pulse versus the prepulse voltage (◆). Holding potential was −90 mV. Resistive linear components were analogically compensated. Oocytes were coexpressing $\alpha_1\beta$ subunits and were injected with 37 nl of 50 mM BAPTA$(Na)_4$. File C2825C08.

Voltage and current dependence of the initial rate of inactivation

The decay of Ca^{2+} currents has a fast and a slow component. As mentioned above, the degree of Ca^{2+}-dependent inactivation was evaluated from the predominant initial fast rate of decay of the Ca^{2+} current because the slow component can be partially attributed to a slow voltage-dependent inactivation also observed in external Ba^{2+} (Fig. 2, *C* and *D*) (Lee et al., 1985; Hadley and Hume, 1987; Campbell et al., 1988; Hadley and Lederer, 1991; Gutnick et al., 1989; Giannattasio et al., 1991). Fig. 4 illustrates the voltage and current dependence of the initial rate of inactivation from an oocyte recorded in the same condition as in Fig. 2 *A*. The initial rate of inactivation correlates positively with the peak Ca^{2+} current amplitude (*filled diamond*) as expected for Ca^{2+}-dependent inactivation and, when plotted with respect to the pulse potential it follows a bell-shaped curve (Fig. 4 *C*, *open diamond*). In addition, the relationship between the initial rate of decay and peak current amplitudes plotted in Fig. 4 *D* (*filled circle*) shows that the same current amplitude is more effective for inducing inactivation at more negative potentials. For example, peak current values are similar at −10 mV and +30 mV, but the rate of inactivation is much faster at −10 mV. Thus, Ca^{2+} entry during channel openings at more negative potentials appears to be more effective than at more depolarized potentials when the flux of Ca^{2+} through single channels is smaller even though the total Ca^{2+} delivered is the same. This interpretation also agrees with the conclusion reached from the experiment in Fig. 2 *E* and is consistent with a process of limited Ca^{2+} diffusion around the channel inner mouth in which the local concentration is governed by the single channel flux (Chad and Eckert, 1984). Below 0 mV, the rate of inactivation becomes slower for more negative test potentials (Fig. 4 *C*), despite the fact that the single channel current should be larger due to an increased driving force. This is the behavior predicted if the channel enters the inactivated state only from the open state, in which case the rate of inactivation depends on the product of the single channel current and the P_o (Sherman et al., 1990).

Differential sensitivity of Cl^- channel activation and Ca^{2+} channel inactivation to cytoplasmic Ca^{2+}

To evaluate the Ca^{2+} sensitivity of the Ca^{2+} inactivation process and Ca^{2+}-induced Cl^- currents, we performed ionic current measurements after injecting different concentrations of BAPTA. Currents in Fig. 5 *A–D* were recorded from $\alpha_1\beta$ injected oocytes bathed in 5 mM external Ca^{2+} either in the presence (96 Cl/5 Ca, *left row*) or absence (0 Cl/5 Ca *right*

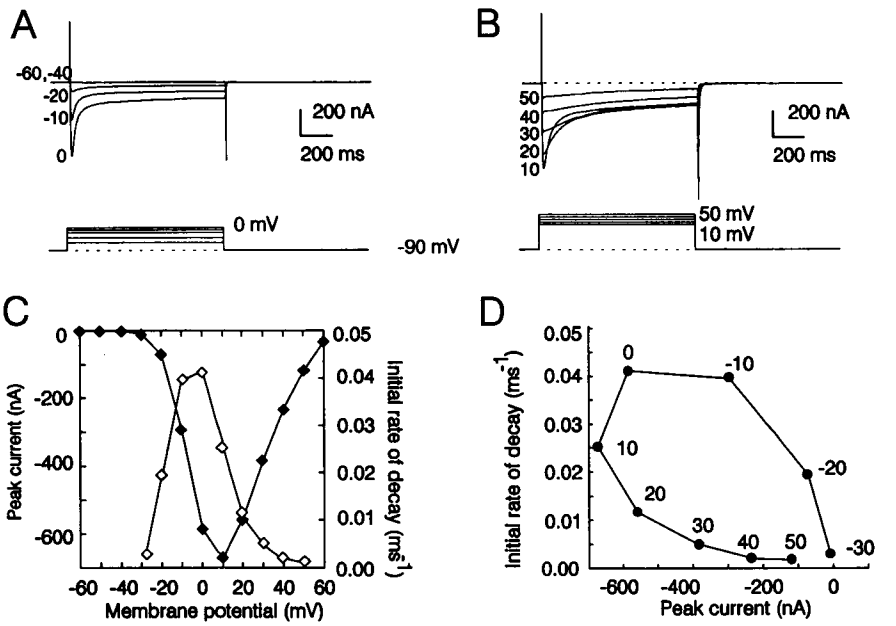

FIGURE 4 The rate of inactivation is Ca^{2+} and voltage-dependent. (*A–B*) Current recordings during 1 s depolarizing steps to the voltage indicated to the left of each trace, in 0 Cl/5 Ca. Holding potential was −90 mV, and pulses had 10 mV voltage increments. Voltages evoking currents of (*A*) increasing amplitudes and (*B*) decreasing amplitudes. Traces were analogically subtracted for linear resistive components. (*C*) Peak current (♦) and initial rate of decay (◇) versus voltage plots. (*D*) Relationship between the initial rate of decay and peak current. The numbers next to the points are the voltages. Note that for peak currents of similar values, the rate of decay is always faster at more negative potentials (e.g., at 30 and −10 mV). Oocytes were coexpressing $\alpha_1\beta$ subunits and were injected with 37 nl of 50 mM BAPTA$(Na)_4$. File C2825C06.

row) of external Cl^-, and injected with different concentrations of Na_4-BAPTA. In external Cl^- (*left row*) Cl^- outward currents were only observed in oocytes injected with 1 and 2.5 mM BAPTA (*A* and *B*; 37 and 93 pmol, respectively). In the absence of external Cl^-, inward Cl^- currents were less evident and became negligible after the injection of 1 mM BAPTA (*A*, *right row*). In contrast to the profound effect of intracellular BAPTA on Ca^{2+}-dependent Cl^- currents, the rate of Ca^{2+} current decay measured in the absence of external Cl^- appeared insensitive to the increase in BAPTA concentrations (2.5–50 mM). This is illustrated by superimposing Ca^{2+} current traces at +20 mV in Cl^--free saline with the injection of different BAPTA concentrations (Fig. 5 *E*).

These experiments demonstrate the virtual elimination of Ca^{2+}-dependent Cl^- currents by reducing cytoplasmic free Ca^{2+} with internal Ca^{2+} buffers (BAPTA), whereas the same maneuver leaves unaffected Ca^{2+}-dependent inactivation, even when using high intracellular BAPTA concentration. These observations indicate that Ca^{2+}-dependent inactivation is less sensitive to Ca^{2+} sequestration by intracellular Ca^{2+} buffers than Ca^{2+}-dependent Cl^- currents. This differential sensitivity of the Ca^{2+} sensors in both channels may either reflect differences in accessibility to BAPTA or in Ca^{2+} affinity.

Ca^{2+} and Ba^{2+} sensitivity of endogenous Cl^- currents in *Xenopus* oocytes

The Ca^{2+} sensitivity of Cl^- channels was further studied in excised inside-out macro-patches from uninjected oocytes.

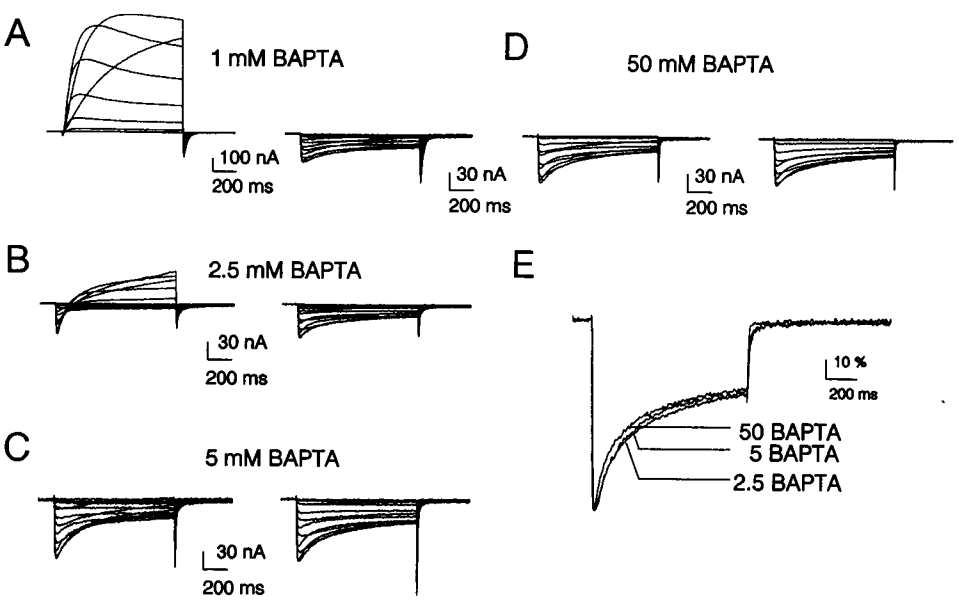

FIGURE 5 The time course of Ca^{2+}-dependent inactivation remains virtually unchanged over a 20-fold range of buffering capacity. (*A–D*) Current traces recorded in 96 Cl/5 Ca (*left* row) or in 0 Cl/5 Ca (*right* row) with BAPTA$(Na)_4$ injected (37 nl) from 1 mM (*A*), 2.5 mM (*B*), 5 mM (*C*), or 50 mM (*D*) stock solutions. Holding potential −90 and 10 mV pulse increments from −60 to 60 mV. Linear resistive components were analogically subtracted. (*E*) Normalized and superimposed from *B*, *C*, and *D* (*right* row) for a pulse to +20 mV and in 0 Cl/5 Ca. Oocytes were coexpressing $\alpha_1\beta$ subunits. Files:
A M3125C03 and M3125C04;
B O3125C02 and O3125C04;
C B3125C04 and B3125C06;
D J3125C06 and J3125C07.

The Ca^{2+} concentration facing the cytoplasmic side was varied from <0.1 mM with 5 mM EGTA to 500 μM Ca^{2+} without EGTA. Cl^- currents were recorded in the presence of a Cl^- gradient (115 mM KCl in the bath; 110 mM KMES, 5 mM NaCl in the pipette). Fig. 6 *A* shows the Ca^{2+} and Ba^{2+} dependence of macroscopic Cl^- currents during voltage pulses from −80 to +80 mV in excised patches. The left arrows in Fig. 6 *A* correspond to the 0 current level and as expected for the Cl^- gradient, Cl^--selective channels induce a steady outward current at 0 mV. Cl^- currents were greatly diminished when the Ca^{2+} concentration was reduced from 100 μM Ca^{2+} (*A1*) to 2 μM (*A2*) and were subsequently activated by 1 mM intracellular Ba^{2+} in the virtual absence of Ca^{2+} (*A3*, EGTA 0.5 mM). The corresponding current-voltage relationships are shown in *B*, and the Cl^- selectivity is shown in *C*. As expected for a Cl^- selective channel, the reduction of the bath Cl^- concentration from 115 mM (NaCl 115 mM) to 5 mM (NaMES 110, NaCl 5) reduced the size of the Cl^- current, and the reversal potential followed the Cl^- gradient, being −75 mV in 115/5 Cl^- (*open square*) and close to 0 in 5/5 mM Cl^- (*filled triangle*).

To obtain an estimate of the Ca^{2+} sensitivity of Ca^{2+}-dependent Cl^- currents, Cl^- current amplitudes at 0 mV were measured at different cytoplasmic Ca^{2+} concentrations and normalized by the current measured in 100 μM Ca^{2+} (Fig. 6 *D*). Pooled data from eight patches were fitted to $I_m = I_{max}/\{1 + (K_{1/2}/[Ca^{2+}])\}^n$, with $K_{1/2}$ = 25.1 μM and the Hill coefficient n = 1.9. The relatively high concentration of Ca^{2+} needed to activate Cl^- current indicates that intracellular Ca^{2+} at the inner membrane surface may reach 10 μM and, thus, relatively low concentrations of BAPTA may be sufficient to reduce the Ca^{2+} levels below the threshold for Cl^- channel activation. On the other hand, the persistency of Ca^{2+}-dependent inactivation with the highest BAPTA concentration used (50 mM) would be consistent with either a Ca^{2+} binding site accessible to the buffer but with high affinity for Ca^{2+}, perhaps in the nanomolar range (Johnson and Byerly, 1993a, b) or a low affinity site close to the Ca^{2+} entry pathway, not readily accessible to intracellular BAPTA. An important difference between these two hypotheses is that the latter predicts that the rate of inactivation should not be influenced by channel density.

Inactivation kinetics is not affected by channel density

One advantage of the *Xenopus* oocyte system is that the density of expressed channels can be varied by performing the current measurements at different times after the mRNA injection. Fig. 7 summarizes the results obtained from eight $\alpha_1\beta$-injected oocytes from the same batch in 5 mM external Ca^{2+} (0 Cl/5 Ca) and measured between 4 and 8 days after mRNA injection. At 0 mV, Ca^{2+} current amplitudes had a sixfold range (−21 to −121 nA). The records in Fig. 7 *A* and the graph in Fig. 7 *B* show that these oocytes with large differences in channel expression had very similar rates of inactivation. These observations indicate that, at least over this range of current density, the rate of Ca^{2+}-dependent inactivation is independent of the channel density, and that it is very unlikely that Ca^{2+} entry through one channel can

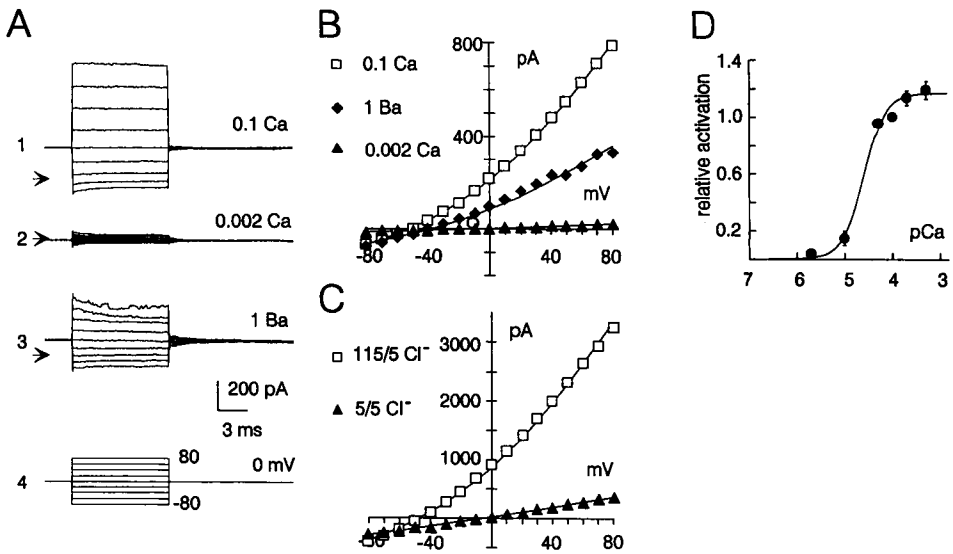

FIGURE 6 Ca^{2+}- and Ba^{2+}-activated Cl^- currents in excised macropatches from uninjected oocytes. (*A*) Current responses to voltage depolarizations from −80 to 80 mV in 10-mV increments from a holding potential of 0 mV. The patch pipette contained KMES 110 mM and NaCl 5 mM. The bath solution facing the cytoplasmic side of the patch was KCl 115 mM with 0.1 mM Ca in *A1* and in the virtual absence of free Ca^{2+} in *A2* (5 mM Na2EGTA). In *A3* 1 mM internal Ba^{2+} in the presence of EGTA 0.5 mM activated Cl− channels. The holding current at 0 mV is the difference between the arrow (0 current) and the current trace at 0 mV. Current-voltage plots for these traces are shown in *B* (□, 0.1 mM Ca^{2+}; ◆, 1 mM Ba^{2+}; ◇, 0.002 mM Ca^{2+}). (*C*) Current-voltage relationship of Ca^{2+}-activated Cl^- currents from an excised patch in the presence of 100 μM Ca^{2+} in 115 mM KCl in the bath (□) and KMESCl⁻5 (▲). (*D*) Ca^{2+} dependence of Cl^- current activation measured as the Cl^- current at 0 mV and at different Ca^{2+} concentrations. Values are mean ±SE from eight patches and were normalized to the current recorded in 100 μM Ca^{2+}. The continuous line shows the fit by a Hill equation with n = 1.91 and $K_{1/2}$ = 25.1 μM. Files: *A* D3714C02, D3714C04, and D3714C05.

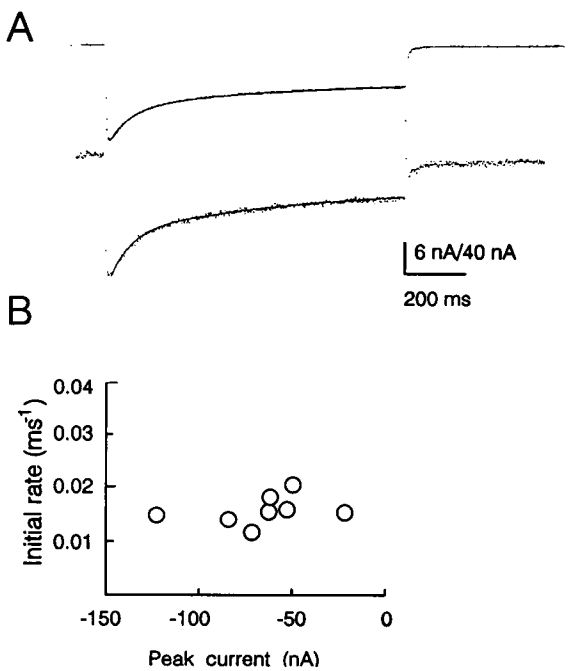

FIGURE 7 The time course of Ca^{2+} current inactivation is insensitive to the level of expression. (*A*) Current recordings in 0 Cl/5 Ca during a depolarization to 0 mV from a holding potential of −90 mV from two oocytes from the same batch that differ by fivefold in their current amplitude (−121 and −21 nA for the *top* and *bottom* traces, respectively). The continuous line is the fit to a dual exponential function of the form $A_f \cdot \exp(-t/\tau_f) + A_s \cdot \exp(-t/\tau_s) + P$, where A_f and A_s are the amplitude factors, τ_f and τ_s are the time constants, and P is the offset. For *top* and *bottom* traces, τ_f = 69 and 67 ms; τ_s = 511 and 595 ms. The initial rate ($1/\tau_f$) for 9 oocytes are plotted with respect to peak current in *B*. The oocytes included in this graph come from a single batch and were coexpressing $\alpha_1\beta$ subunits. They were injected with 37 nl of 50 mM BAPTA$(Na)_4$. File: *A* C3604C02; *B* B3609C02.

interact with neighboring channels to induce inactivation. More likely, the main component of inactivation arises from the Ca^{2+} flowing through a single channel protein and acting on the same channel.

Expression of α_1 subunit alone is sufficient for Ca^{2+}-dependent inactivation

Coexpression of the β cardiac Ca^{2+} channel subunit, together with the channel forming α_1 subunit, increased the rate of channel opening and current size while shifting to more negative potential the P_o-voltage curve (Varadi et al., 1991; Wei et al., 1991; Perez Reyes et al., 1992; Neely et al., 1993). We investigated whether the potential binding site responsible for the Ca^{2+}-dependent inactivation is located either in the α_1 or the β subunit. Peak inward currents from oocytes injected with α_1 mRNA alone are roughly one-fifth of those recorded when both subunits mRNA were injected. In most cases, peak currents were less than 20 nA at +20 mV in 5 mM Ca^{2+}. In addition, the voltage dependence of activation is shifted by about 20 mV with respect to $\alpha_1\beta$ expressing oocytes (Neely et al., 1993). As a consequence, in oocytes injected with α_1 subunit alone Ca^{2+} currents are smaller in amplitude and inactivate at a slower rate making a detailed study of Ca^{2+}-dependent inactivation difficult. Nevertheless, we were able to demonstrate the presence of Ca^{2+}-dependent inactivation in oocytes injected with the α_1 subunit alone (Fig. 8).

Fig. 8 shows Ca^{2+} currents recorded from an oocyte expressing the cardiac α_1 subunit alone before (*A*) and after (*B*) the addition of the Ca^{2+} channel agonist 500 nM (−)-BayK-8644. Records in *C* show superimposed traces obtained in 5 mM Ca^{2+} and then in 10 mM Ba^{2+}. These experiments demonstrate that inactivation was eliminated after replacing 5 mM Ca^{2+} with 10 mM Ba^{2+} and, therefore, the cardiac β subunit was not required for Ca^{2+}-dependent inactivation. For a test pulse to 30 mV, the addition of BayK-8644 increased peak current amplitude from 16 to 42 nA and the rate of Ca^{2+} current decay from 1.4 to 2.6 s^{-1}. The BayK-8644 increase of 2.6-fold in peak current amplitude and 1.9-fold in the rate of decay can be explained by the local domain model proposed by Sherman et al. (1990).

DISCUSSION

The evidence presented here shows that the cloned α_1 pore-forming subunit of the cardiac Ca^{2+} calcium channel expressed in *Xenopus* oocytes undergoes Ca^{2+}-dependent inactivation and that this process can be measured successfully after eliminating Ca^{2+}-dependent Cl^- currents by the intracellular injection of the Ca^{2+} chelator BAPTA. This prevents the activation of the endogenous Cl^- channels, which require about 20 mM cytoplasmic free Ca^{2+} to reach 50% activation

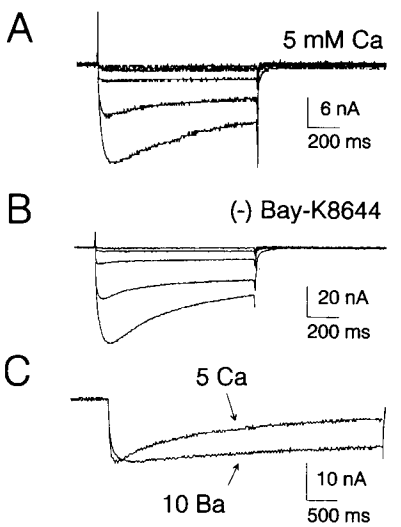

FIGURE 8 The cardiac α_1 subunit alone is sufficient for Ca^{2+}-induced inactivation. Current traces in 0 Cl/5 Ca in control conditions (*A*) and after the addition of Bay-K8644 (500 nM) (*B*) Pulses from −50 to 30 mV in 20-mV increments from −90 mV holding potential. (*C*) Superimposed current traces from the same oocyte in 500 nM (−)BayK-8644 during a long pulse to 0 mV in 0 Cl/5 Ca and 0 Cl/10 Ba. Note the absence of inactivation in 10 mM Ba^{2+}. The oocytes were expressing the cardiac α_1 subunit alone and were injected with 37 nl of 50 mM $(Na)_4$BAPTA. Files: *A* F2022C03; *B* F2022C08; *C* F2022C09.

(Fig. 6 *D*). Single channel activity of oocytes' Ca^{2+}-dependent Cl^- currents has been recorded using 10 μM internal Ca^{2+} (Methfessel et al., 1986; Takahashi et al., 1987). This low sensitivity to Ca^{2+} is consistent with the suppression of macroscopic Cl^- currents with low concentrations of BAPTA. It may also explain their lack of saturation with increases in extracellular Ca^{2+} in oocytes pretreated with a Ca^{2+} ionophore (Boton et al., 1989) and the discrepancy between the maximal Cl^- currents evoked by membrane depolarization or Ca^{2+} injection (Miledi and Parker, 1984). An additional finding is that Ba^{2+}, in the millimolar range, can also activate these Cl^- channels and, therefore, the substitution of Ca^{2+} by Ba^{2+} is insufficient for the isolation of currents going through Ca^{2+} channels.

The rate of inactivation reported here is slower than that reported for cardiac cells, in either frog (Campbell et al., 1988; Argibay et al., 1988) or mammalian preparations (Josephson et al., 1984; Hartzell and White, 1989). Additional Ca^{2+} channel subunits or regulatory enzymes missing in the oocytes may partially explain this difference together with a different micro-environment surrounding the channel. For instance, in heart, Ca^{2+} channels are associated to the Ca^{2+} release sites that are coupled to Ca^{2+} influx (Stern, 1992). Also, it seems that in native tissue the mean distance between channels is such that Ca^{2+} entering through one channel can inactivate nearby channels (Imredy and Yue, 1992).

The time course of inactivation observed here compares well with Ca^{2+} currents of pancreatic β-cells recorded in the presence of internal 10 mM EGTA or 7 mM BAPTA (Plant, 1988). In this system, the inactivation process was modeled in terms of local domains where Ca^{2+} affects only the channel from which it enters, and the local concentration is mostly determined by the flux of Ca^{2+} through single channels (Sherman et al., 1990). This model predicts that the rate of inactivation is faster at more negative potentials when there is a larger Ca^{2+} flux through single channels. The local domain hypothesis is favored by the following properties of the initial rate of Ca^{2+} inactivation in expressed cardiac Ca^{2+}-channel: 1) it was faster at more negative potentials for an equivalent Ca^{2+} current amplitude; 2) it was faster in 10 mM than 2 mM external Ca^{2+}, and specifically, when measured at 10 mV when the Ca^{2+} current had a similar amplitude in both Ca^{2+} concentrations; 3) it was unaffected for a 10-fold change in internal BAPTA; and 4) it was relatively independent on the level of channel expression. Furthermore, the higher sensitivity of Ca^{2+}-dependent Cl^- channels to internal Ca^{2+} buffers than to the Ca^{2+}-dependent inactivation process can also be explained by the local domain hypothesis, in which expressed Ca^{2+} channels and endogenous Cl^- channels are sensing different Ca^{2+} compartments. The fact that the potentiation by the Ca^{2+} channel agonist BayK-8644 did not result in a comparable effect on the rate of inactivation also argues against an inactivation process governed by Ca^{2+} accumulation. Finally, we have also shown that the inactivation by intracellular Ca^{2+} occurs when the pore-forming α_1 subunit is expressed alone and, therefore, the primary Ca^{2+} binding structure is not located in the β subunit.

We thank G. Schuster and W.-Q. Dong for injection of the *Xenopus* oocytes and Dr. Ligia Toro for helpful suggestions during the preparation of the manuscript.

This work was supported by a National Research Service Award to A. Neely and grants AR38970 to E. Stefani and HL37044 to L. Birnbaumer and E. Stefani from the National Institute of Health.

REFERENCES

Argibay, J. A., R. Fischmeister, and H. C. Hartzell. 1988. Inactivation, reactivation and pacing dependence of calcium current in frog cardiocytes: correlation with current density. *J. Physiol. (Lond.)*. 401: 201–226.

Barish, M. E. 1983. A transient calcium-dependent chloride current in the immature *Xenopus* oocyte. *J. Physiol. (Lond.)*. 342:309–325.

Bean, B. P. 1989. Classes of calcium channels in vertebrate cells. *Annu. Rev. Physiol.* 51:367–384.

Bertolino, M., and R. R. Llinas. 1992. The central role of voltage-activated and receptor-operated calcium channels in neuronal cells. *Annu. Rev. Pharmacol. Toxicol.* 32:399–421.

Boton, R., N. Dascal, B. Gillo, and Y. Lass. 1989. Two calcium-activated chloride conductances in *Xenopus laevis* oocytes permeabilized with the ionophore A23187. *J. Physiol. (Lond.)*. 408:511–534.

Brehm, P., and R. Eckert. 1978. Calcium entry leads to inactivation of calcium channel in *Paramecium*. *Science*. 202:1203–1206.

Campbell, D. L., W. R. Giles, J. R. Hume, and E. F. Shibata. 1988. Inactivation of calcium current in bull-frog atrial myocytes. *J. Physiol. (Lond.)*. 403:287–315.

Carafoli, E. 1993. Intracellular Calcium homeostasis. *Annu. Rev. Biochem.* 56:395–433.

Castellano, A., X. Wei, L. Birnbaumer, and E. Perez Reyes. 1993. Cloning and expression of a third calcium channel beta subunit. *J. Biol Chem.* 268:3450–3455.

Chad, J. 1989. Inactivation of calcium channels. *Comp. Biochem. Physiol.* 93:95–105.

Chad, J., and R. Eckert. 1984. Calcium domains associated with individual channels can account for anomalous voltage relations of Ca-dependent responses. *Biophys. J.* 45:993–999.

Chad, J., and R. Eckert. 1986. An enzymatic mechanism for calcium current inactivation in dialysed Helix neurones. *J. Physiol. (Lond.)*. 378:31–51.

Eckert, R., and J. Chad. 1984. Inactivation of Ca channels. *Prog. Biophys. mol. Biol.* 44:261–267.

Eckert, R., and D. Tillotson. 1981. Calcium-mediated inactivation of the calcium conductance in caesium-loaded giant neurones of *Aplysia californica*. *J. Physiol. (Lond.)*. 314:265–280.

Fabiato, A. 1988. Computer programs for calculating total from specified free or free from specified total ionic concentrations in aqueous solutions containing multiple metal and ligands. *Methods Enzymol.* 157:378–417.

Giannattasio, B., S. W. Jones, and A. Scarpa. 1991. Calcium currents in the A7r5 smooth muscle-derived cell line. Calcium-dependent and voltage-dependent inactivation. *J. Gen. Physiol.* 98:987–1003.

Gutnick, M. J., H. D. Lux, D. Swandulla, and H. Zucker. 1989. Voltage-dependent and calcium-dependent inactivation of calcium channel current in identified snail neurones. *J. Physiol.* 412:197–220.

Hadley, R. W., and J. R. Hume. 1987. An intrinsic potential-dependent inactivation mechanism associated with calcium channels in guinea-pig myocytes. *J. Physiol. (Lond.)*. 389:205–222.

Hadley, R. W., and W. J. Lederer. 1991. Ca^{2+} and voltage inactivate Ca^{2+} channels in guinea-pig ventricular myocytes through independent mechanisms. *J. Physiol. (Lond.)*. 444:257–268.

Hartzell, H. C., and R. E. White. 1989. Effects of magnesium on inactivation of the voltage-gated calcium current in cardiac myocytes. *J. Gen. Physiol.* 94:745–767.

Imredy, J. P., and D. T. Yue. 1992. Submicroscopic Ca^{2+} diffusion mediates inhibitory coupling between individual Ca^{2+} channels. *Neuron.* 9: 197–207.

Johnson, B. D., and L. Byerly. 1993a. Photo-released intracellular Ca^{2+} rapidly blocks Ba^{2+} current in Lymnaea neurons. *J. Physiol. (Lond.).* 462:321–347.

Johnson, B. D., and L. Byerly. 1993b. A cytoskeletal mechanism for Ca^{2+} channel metabolic dependence and inactivation by intracellular Ca^{2+}. *Neuron.* 10:797–804.

Josephson, I. R., J. Sanchez-Capula, and A. M. Brown. 1984. A comparison of calcium currents in rat and guinea pig single ventricular cells. *Circ. Res.* 54:144–156.

Kalman, D., P. H. OLague, C. Erxleben, and D. L. Armstrong. 1988. Calcium-dependent inactivation of the dihydropyridine-sensitive calcium channels in GH3 cells. *J. Gen. Physiol.* 92:531–548.

Keizer, J., and L. W. Maki. 1992. Conditional probability analysis for a domain model of Ca^{2+}-inactivation of Ca^{2+} channels. *Biophys. J.* 63: 291–295.

Kostyuk, P. G. 1992. Calcium Ions in Nerve Cell Function. Oxford University Press, New York.

Lee, K. S., E. Marban, and R. W. Tsien. 1985. Inactivation of calcium channels in mammalian heart cells: joint dependence on membrane potential and intracellular calcium. *J. Physiol. (Lond.).* 364:395–411.

Llinas, R., M. Sugimori, and R. B. Silver. 1992. Microdomains of high calcium concentration in a presynaptic terminal. *Science.* 256:677–679.

Methfessel, C., V. Witzemann, T. Tkahashi, M. Mishina, S. Numa, and B. Sakmann. 1986. Patch clamp measurements on *Xenopus laevis* oocytes: currents through endogenous channels and implanted acetylcholine receptor and sodium channels. *Pflugers Arch.* 407:577–588.

Miledi, R. 1982. A calcium-dependent outward current in *Xenopus laevis* oocytes. *Proc. R. Soc. Lond. B Biol. Sci.* 215:492–497.

Miledi, R., and I. Parker. 1984. Chloride current induced by injection of calcium in *Xenopus* oocytes. *J. Physiol. (Lond.).* 357:173–183.

Neely, A., X. Wei, R. Olcese, L. Birnbaumer, and E. Stefani. 1993. Cardiac β subunit facilitates α_1 Ca channel opening without changes in the voltage sensor. *Science.* 262:575–578.

Perez Reyes, E., A. Castellano, H. S. Kim, P. Bertrand, E. Baggstrom, A. E. Lacerda, X. Y. Wei, and L. Birnbaumer. 1992. Cloning and expression of a cardiac/brain beta subunit of the L-type calcium channel. *J. Biol. Chem.* 267:1792–1797.

Plant, T. D. 1988. Properties and calcium-dependent inactivation of calcium currents in cultured mouse pancreatic B-cells. *J. Physiol. (Lond.).* 404: 731–747.

Sherman, A., J. Keizer, and J. Rinzel. 1990. Domain model for Ca^{2+}-inactivation of Ca^{2+} channels at low channel density. *Biophys. J.* 58: 985–995.

Simon, S. J., and R. Llinas. 1985. Compartmentalization of the submembrane calcium activity during calcium influx and its significance in transmitter release. *Biophys. J.* 48:485–498.

Standen, N. B., and P. R. Stanfield. 1982. A binding-site model for calcium channel inactivation that depends on calcium entry. *Proc. R. Soc. Lond. B Biol. Sci.* 217:101–110.

Stern, M. D. 1992. Buffering of calcium in the vicinity of a channel pore. *Cell Calcium.* 13:183–192.

Taglialatela, M., L. Toro, and E. Stefani. 1992. Novel voltage clamp to record small, fast currents from ion channels expressed in *Xenopus* oocytes. *Biophys. J.* 61:78–82.

Takahashi, T., E. Neher, and B. Sakmann. 1987. Rat brain serotonin receptors in *Xenopus* oocytes are coupled by intracellular calcium to endogenous channels. *Proc. Natl. Acad. Sci. USA.* 84:5063–5067.

Tillotson, D. 1979. Inactivation of calcium conductance dependent on entry of calcium ions in molluscan neurons. *Proc. Natl. Acad. Sci. USA.* 76: 1497–1500.

Varadi, G., P. Lory, D. Schultz, M. Varadi, and A. Schwartz. 1991. Acceleration of activation and inactivation by the beta subunit of the skeletal muscle calcium channel. *Nature.* 352:159–162.

Wei, X. Y., E. Perez Reyes, A. E. Lacerda, G. Schuster, A. M. Brown, and L. Birnbaumer. 1991. Heterologous regulation of the cardiac Ca^{2+} channel alpha 1 subunit by skeletal muscle beta and gamma subunits. Implications for the structure of cardiac L-type Ca^{2+} channels. *J. Biol. Chem.* 266:21943–21947.